# The GAP arginine finger movement into the catalytic site of Ras increases the activation entropy

Carsten Kötting[†], Angela Kallenbach[†], Yan Suveyzdis[†], Alfred Wittinghofer[‡], and Klaus Gerwert[†§]

[†]Lehrstuhl für Biophysik, Ruhr-Universität Bochum, D-44780 Bochum, Germany; and [‡]Max-Planck-Institut für Molekulare Physiologie, Otto-Hahn-Strasse 11, 44227 Dortmund, Germany

Edited by Robert H. Austin, Princeton University, Princeton, NJ, and approved February 14, 2008 (received for review December 28, 2007)

**Members of the Ras superfamily of small G proteins play key roles in signal transduction pathways, which they control by GTP hydrolysis. They are regulated by GTPase activating proteins (GAPs). Mutations that prevent hydrolysis cause severe diseases including cancer. A highly conserved ''arginine finger'' of GAP is a key residue. Here, we monitor the GTPase reaction of the Ras·RasGAP complex at high temporal and spatial resolution by time-resolved FTIR spectroscopy at 260 K. After triggering the reaction, we observe as the first step a movement of the switch-I region of Ras from the nonsignaling ''off'' to the signaling ''on'' state with a rate of 3 $s^{-1}$. The next step is the movement of the ''arginine finger'' into the active site of Ras with a rate of $k_2$ = 0.8 $s^{-1}$. Once the arginine points into the binding pocket, cleavage of GTP is fast and the protein-bound $P_i$ intermediate forms. The switch-I reversal to the ''off'' state, the release of $P_i$, and the movement of arginine back into an aqueous environment is observed simultaneously with $k_3$ = 0.1 $s^{-1}$, the rate-limiting step. Arrhenius plots for the partial reactions show that the activation energy for the cleavage reaction is lowered by favorable positive activation entropy. This seems to indicate that protein-bound structured water molecules are pushed by the ''arginine finger'' movement out of the binding pocket into the bulk water. The proposed mechanism shows how the high activation barrier for phosphoryl transfer can be reduced by splitting into partial reactions separated by a $P_i$-intermediate.**

enzyme catalysis | FTIR spectroscopy | GTPases | phosphate | proteins

In a eukaryotic cell, ≈150 different GTP-binding (G) proteins control various cellular functions by acting as molecular switch devices (1). The active conformation, the ''on'' state, is induced by GTP-binding, whereas hydrolysis to GDP and $P_i$ induces the inactive ''off'' conformation. The catalysis of GTP hydrolysis by the small G protein Ras serves as a prototype for the hydrolysis reaction of small G proteins. Its detailed understanding thus seems paradigmatic for the GTPase reaction mechanisms of many Ras superfamily members (2), although other mechanisms have also been described (3). Ras activates several signal transduction pathways; the most prominent of which are directed toward Raf/MEK/Erk, PI (3) kinase, and RalGDS (3).

The intrinsic GTPase reaction of Ras is slow, with $4.7 \times 10^{-4}$ $s^{-1}$ at 37°C, but Ras-specific GTPase activating proteins (RasGAPs, GAPs from now) (4) catalyze the reaction ≈$10^5$-fold to 19 $s^{-1}$ (measured at 25°C) (5) and thereby control the Ras switch. The oncogenic mutants of Ras can still bind GTP and interact with GAP, but the intrinsic GTP hydrolysis is impaired and is no longer catalyzed by GAP. This contributes to uncontrolled proliferation and eventually tumor formation. Ras oncogenes are found in 20% of all human tumors (6), whereas the RasGAPs neurofibromin is found mutated and deleted in the benign tumor type neurofibromatosis but is also found, albeit less frequently, in solid tumors (5). More weakly activating alleles of K-Ras with impaired GTP hydrolysis capacity have recently been found in developmental disorders such as Noonan syndrome (7). The GTPase reaction thus represents a valuable target for antidisease therapy. This would, however, require a detailed mechanistic and structural insight into the GAP-mediated catalysis as a prerequisite for a rational drug development (8).

The key residue for GAP-mediated catalysis is the so-called ''arginine finger'' (9). In the x-ray structure of the Ras·GDP·$AlF_3$·RasGAP complex mimicking the transition state, it points into the GTP binding site of Ras. It stabilizes the position of the catalytic Gln-61 and neutralizes negative charge on the phosphates (10). The catalytic arginine finger is a highly conserved motive among several GAP proteins for small G proteins (11). The participation of an arginine in phosphoryl transfer as seen in the Ras-GAP system is thus paradigmatic because it is also observed in other transition state analogue structures such as the $\alpha$-subunit of large G proteins (12), in the signal recognition particles (13, 14), and even in ATP-binding proteins such as F1-ATPase, where an arginine from the $\alpha$-subunit points into the $\beta$-subunit active site (15). From these structures it is not yet clear whether the arginine finger is also required for the Ras·GTP·GAP ground state complex or whether GAP binding and arginine movement are separate, consecutive steps in the hydrolysis reaction. In the case of RhoGAP, it has been shown that the arginine finger is pointing away from the active site in ground state complex, whereas it is pointing toward the phosphates in the $AlF_x$ complex (16, 17).

One important function of GAP is the stabilization of the orientation of Gln-61 by an H-bond to the arginine backbone carbonyl. Gln-61 positions a water molecule for in-line nucleophilic attack on the $\gamma$-phosphate. However, the influence of the arginine finger on the charge distribution in GTP is not resolved by the x-ray crystallography. Based on time-resolved (tr) FTIR experiments, it is proposed that a charge shift toward the $\beta$-phosphate induced by GAP is crucial for catalysis (18, 19). The charge distribution in GTP in the Ras·GTP·GAP ground state is more GDP product-like compared with GTP in water (20). Thereby, the free activation energy is reduced. The catalysis by Ras itself is shown to be mainly caused by a reduction of the activation enthalpy due to charge movements (21). This confirms the importance of the protein-induced charge distribution in GTP for catalysis. Elucidating a possible arginine movement during catalysis and its impact on the GTP charge distribution is therefore of eminent interest for a full understanding of GAP-mediated catalysis.

trFTIR spectroscopy might allow monitoring both a possible movement of the arginine finger and its effect on charge distribution. By trFTIR, a strongly protein-bound $H_2PO_4^-$ ($P_i$) has recently been identified as an intermediate in the GAP-catalyzed GTPase reaction (22). The protein-bound $P_i$ is formed

Author contributions: C.K. and K.G. designed research; A.K. and Y.S. performed research; A.W. contributed new reagents/analytic tools; C.K., A.K., Y.S., and K.G. analyzed data; and C.K., A.W., and K.G. wrote the paper.

The authors declare no conflict of interest.

This article is a PNAS Direct Submission.

§To whom correspondence should be addressed. E-mail: gerwert@bph.rub.de.

This article contains supporting information online at www.pnas.org/cgi/content/full/0712095105/DCSupplemental.

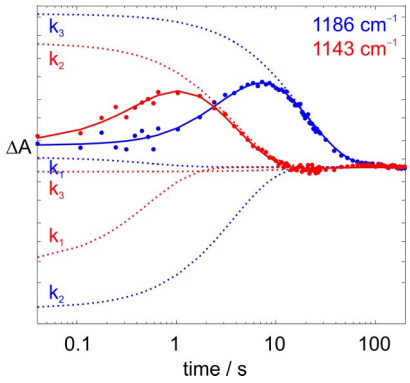


**Fig. 1.** Time-dependent absorbance changes of a marker band of the protein-bound phosphate at 1,186 $cm^{-1}$ as described in ref. 22 (blue). The time-dependent absorbance changes at 1,143 $cm^{-1}$ (red) increase with $k_1$, the formation of the newly resolved state, and decrease with $k_2$, the formation of the protein-bound phosphate. The amplitudes of the global fit with the three exponential rates for positive (increasing) and negative (decreasing) changes are given as dotted lines.

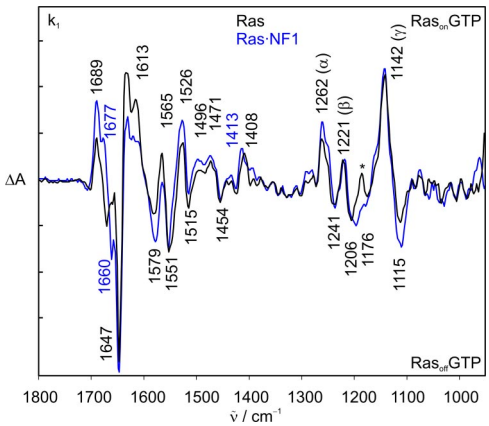


**Fig. 2.** Amplitude spectra of rate 1, the $Ras_{off}GTP \rightarrow Ras_{on}GTP$ conformational change, for Ras (26) (black) and Ras·GAP (blue). Bands facing downward belong to the $Ras_{off}GTP$ state; bands facing upward are from the $Ras_{on}GTP$ state. The asterisk denotes an artifact that is present in some of our measurements, independent of the presence of GAP.

in a reversible reaction before it is released in the rate-limiting step. The GTPase reaction is commonly started by a laser flash, using photolabile caged GTP. Here, *para*-hydroxyphenacyl (pHP)-GTP, instead of nitrophenylethyl (NPE)-GTP, is used because the release of GTP is much faster: 500 ps in contrast to ≈500 ms (23, 24). This now allows possible reaction steps preceding catalysis to be monitored. In combination with $^{15}N$ isotopic labeling of the RasGAP neurofibromin (7), we can now better resolve individual steps of the reaction pathways and study the contribution of GAP residues in a time-dependent manner. Using Arrhenius analysis, we also determined thermodynamic parameters and their implications for catalysis.

## Results and Discussion

Infrared difference spectroscopy monitors in a temporally resolved manner at atomic detail the reaction of individual residues or ligands within a protein, by subtracting infrared spectra at different time points of the reaction from the reference spectrum before the reaction. The difference spectra select the absorbance bands of reactive residues from the background absorbance. The spectra are taken with 10-ms time resolution. By a global fit method (25), the corresponding amplitude spectra and apparent rates can be obtained. The amplitude spectra show the spectral changes in each of the consecutive steps of the reaction. The infrared absorbance bands are assigned unequivocally to the respective residues by either isotopic labeling of the residue of interest or exchange of the residue by site-directed mutagenesis. This leads to either a frequency shift or a disappearance of the residue band in question as compared with the corresponding band in the WT spectrum. Thereby, the reactions of individual residues can be followed simultaneously during GTP hydrolysis.

The absorbance changes after photolysis of caged GTP bound to Ras·GAP can be described by three apparent rates, $k_1 = 3\ s^{-1}$, $k_2 = 0.8\ s^{-1}$, and $k_3 = 0.1\ s^{-1}$. In Fig. 1, the absorbance changes of two typical marker bands are shown. The band at 1,186 $cm^{-1}$ represents the protein-bound $H_2PO_4^-$ ($P_i$) (blue). As described recently (22), this species appears with $k_2 = 0.8\ s^{-1}$ (bond breakage) and decays with $k_3 = 0.1\ s^{-1}$ ($P_i$ release). In earlier publications, $k_1$ described the formation of GTP from NPE-caged GTP, which is slower than the process observed here. The pHP-caged GTP used here forms GTP within 500 ps after photolysis, much faster than it takes to record the first spectrum (≈40 ms) (23, 24). Thus, we now observe with $k_1$ an additional process of the Ras·GAP system that was masked by the slow caged compound in earlier measurements. An absorbance change due to this process is shown in Fig. 1 (red), where a species is forming with $k_1$ after photolysis and decaying with the appearance of the protein-bound $P_i$.

**Conformational Change with $k_1$.** Ras in complex with caged GTP is in the "off" conformation. After photolysis of caged GTP, $Ras_{off}GTP$ is formed and, subsequently, a conformational change to $Ras_{on}GTP$ occurs with a rate of $5 \pm 1\ s^{-1}$ (26). This is very similar to the $k_1$ rate of $3 \pm 2\ s^{-1}$ we now observe in the Ras-GAP system after photolysis. Amplitude spectra of the apparent rate constants are characteristic for the biochemical process they describe. Comparison of the Ras-GAP $k_1$ amplitude spectra with the corresponding spectrum of Ras alone obtained earlier (26) shows an overall agreement (Fig. 2), demonstrating that they reflect a very similar process. The overall agreement shows, furthermore, that only minor or few interactions between GAP and Ras occur with $k_1$. Both GTP bands between 1,300 $cm^{-1}$ and 1,100 $cm^{-1}$ and the protein conformational sensitive amide bands between 1,690 $cm^{-1}$ and 1,620 $cm^{-1}$, and 1,580 $cm^{-1}$ and 1,540 $cm^{-1}$ are similar. Only small differences are observed at 1,677/1,660 $cm^{-1}$ and 1,408 $cm^{-1}$. From the overall agreement, we conclude that $k_1$ in the Ras-GAP reaction describes the $Ras_{off}GTP$ to $Ras_{on}GTP$ process. The reaction scheme shown as Scheme 1 can thus be deduced.

**Ras·GAP Interaction with $k_1$.** To identify the contribution of the GAP protein in the individual reaction steps, the GAP domain of NF1 was fully labeled with $^{13}C$ and $^{15}N$ ($U\text{-}^{13}C^{15}N$). Thus, all bands arising from GAP should shift, whereas all bands from Ras, because it is unlabeled, should remain unchanged. In Fig.

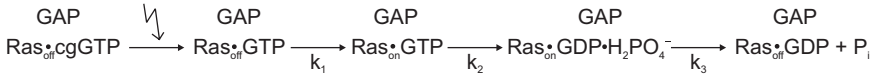


**Scheme 1.**

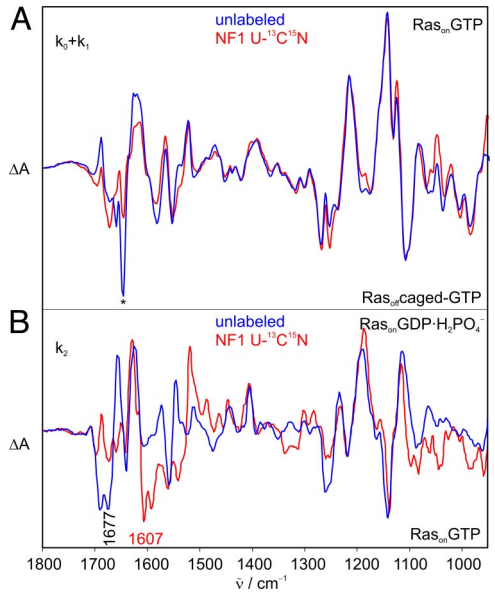


**Fig. 3.** Comparison of the amplitude spectra of the GTPase reaction of the Ras·GAP complex using unlabeled and U-$^{13}C^{15}N$-labeled GAP. (*A*) Amplitude spectra of the sum of photolysis plus rate 1 for the GTPase reaction of the Ras·GAP complex. Unlabeled NF1 was used for the blue spectrum, and U-$^{13}C^{15}N$-labeled NF1 was used for the red spectrum. Bands facing downward are from the disappearing $Ras_{off}$caged-GTP state; bands facing upward are from the appearing $Ras_{on}GTP$ state. (*B*) Amplitude spectra of rate 2 for the GTPase reaction of the Ras·GAP complex. The blue spectrum is from measurements using unlabeled NF1, and the red spectrum is from measurements using U-$^{13}C^{15}N$-labeled NF1. Bands facing downward are from the $Ras_{on}GTP$ state; bands facing upward belong to the $Ras_{on}GDP{\cdot}H_2PO_4^-$ state. In this rate, distinct shifts are observed, indicating a strong participation of the GAP. The asterisk denotes an artifact band that is present in some of our measurements due to the bad signal-to-noise ratio in this region.

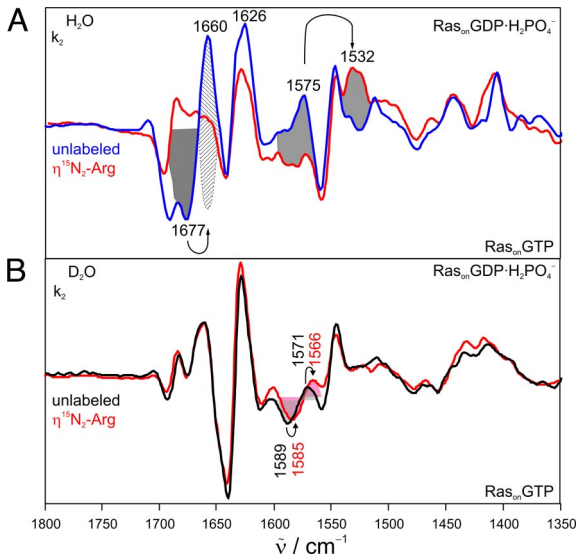


**Fig. 4.** Comparison of the amplitude spectra of the GTPase reaction of the Ras·GAP complex using unlabeled and $\eta^{15}N_2$-Arg labeled GAP. (*A*) Amplitude spectra of rate 2 for the GTPase reaction of the Ras·GAP complex. The blue spectrum is from measurements using unlabeled GAP, and the red spectrum is from measurements using $\eta^{15}N_2$-Arg-labeled GAP. Bands facing downward are from the $Ras_{on}GTP$ state; bands facing upward belong to the $Ras_{on}GDP{\cdot}H_2PO_4^-$ state. The band at 1,677 $cm^{-1}$ can be assigned to arginine in a water environment; the band at 1,575 $cm^{-1}$ can be assigned to arginine within the binding pocket. (*B*) Amplitude spectra of rate 2 for the GTPase reaction of the Ras·GAP complex in $D_2O$. The black spectrum is from measurements using unlabeled GAP, and the red spectrum is from measurements using $\eta^{15}N_2$-Arg-labeled GAP. Bands facing downward are from the $Ras_{on}GTP$ state; bands facing upward belong to the $Ras_{on}GDP{\cdot}H_2PO_4^-$ state. The band at 1,589 $cm^{-1}$ can be assigned to arginine in a deuterated water environment; the band at 1,571 $cm^{-1}$ can be assigned to arginine within the binding pocket.

3*A*, we show the difference spectra of $Ras_{off}$cagedGTP and $Ras_{on}GTP$. This is obtained by adding the amplitude spectra of the photolysis and the $k_1$ reaction. Thereby, processes faster than $k_1$ also are observed, and the signal-to-noise ratio, in addition, is much better than in the amplitude spectrum of $k_1$ alone. Because only minor differences between the spectra with unlabeled GAP and U-$^{13}C^{15}N$-labeled GAP are observed, we conclude that GAP plays no role in the "off" to "on" transition of the Ras protein. This confirms the conclusions drawn above from the agreement of the $k_1$ amplitude spectra of Ras and Ras-GAP in Fig. 2.

**Ras·GAP Interaction with $k_2$.** In contrast to the photolysis plus $k_1$ amplitude spectra for the "off" to "on" reaction, the hydrolysis amplitude spectra $k_2$ (Fig. 3*B*) reveal remarkable frequency shifts due to the $^{13}C^{15}N$ GAP labeling. Because $k_2$ reflects the bond breakage, the GAP interaction is expected to be crucial in this reaction step. Because we suspected that the arginine finger plays a crucial role in this step, we expressed NF1 in which the two ηN atoms of the arginines were group specifically labeled by $^{15}N$. The guanidinium group has two strong $\nu(CN_3H_5^+)$ bands at ≈1,672 $cm^{-1}$ and 1,635 $cm^{-1}$ (27). Indeed, the $k_2$ amplitude spectrum shows a clear band-shift in this region (Fig. 4*A*). The band at 1,677 $cm^{-1}$ is shifted by ≈17 $cm^{-1}$ to 1,660 $cm^{-1}$ due to $\eta^{15}N_2$-arginine labeling. The shifted negative band compensated the positive band at 1,660 $cm^{-1}$, resulting in no net absorbance change as indicated by the marked areas. The frequency is in the expected region of an arginine vibration in an aqueous environment. Furthermore, it shows the expected isotopic shift of guanidinium according to density functional theory (DFT) calculations [supporting information (SI) *Experimental Procedures*]. Thus, the band at 1,677 $cm^{-1}$ can be clearly assigned to an arginine in an aqueous environment. In addition, a positive band at 1,575 $cm^{-1}$ is shifted to 1,532 $cm^{-1}$. The band position clearly deviates from the band position of arginine in water and is expected for arginine within proteins (28, 29). Therefore, this band is assigned to an arginine in a protein environment, and we conclude that the band-shift reflects the movement of arginine from an aqueous environment into the protein binding pocket. Considering that an arginine is crucial for the phosphoryl transfer and that $k_2$ describes an arginine movement, the most likely conclusion is that it is Arg-1276 of NF1, the arginine finger, that is relocated into the active site.

Because the band at 1,677 $cm^{-1}$ overlaps with the strong amide I and water bands, it is less appropriate for a kinetic analysis. Therefore, we performed the experiments in $D_2O$ (Fig. 4*B*). The guanidinium band is shifted to 1,589 $cm^{-1}$. Such a large shift in $D_2O$ is in agreement with shifts observed in a model compound (Fig. S1) and DFT calculations (Fig. S2 and Table S1). The small shift obtained by $\eta^{15}N_2$ labeling also agrees with the model compound and DFT calculations. In $D_2O$ the complete band reflects only an arginine vibration. Thus, the whole band at 1,589 $cm^{-1}$ without any overlap of other residues is assigned to arginine. Its absorbance change can be used as a reliable marker band for the arginine movement.

**Kinetics for the Switch-I and Arginine Movements as Compared with the Hydrolysis Reaction.** The assignments of the bands of the key residues now allow monitoring of the kinetics of their absorbance changes (Fig. 5). The marker band at 1,684 $cm^{-1}$ (Fig. 5*A*) reflects the movement of Thr-35 (26) and the conformational change of

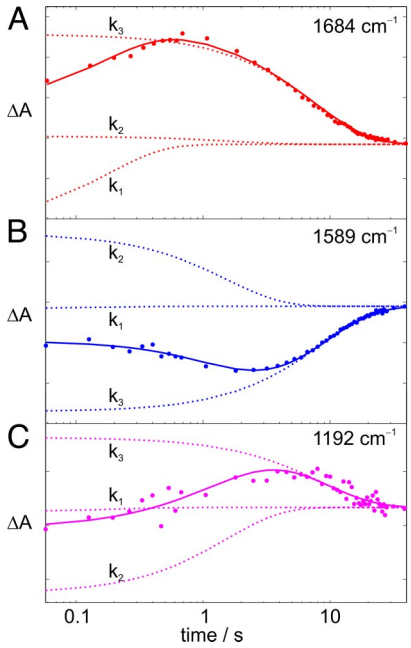


**Fig. 5.** Time-dependent absorbance changes during the GTPase reaction of Ras·GAP. (*A*) Time-dependent absorbance changes of a marker band (in $D_2O$) for Thr-35 of switch I of Ras as described in ref. 26. The amplitudes of the global fit with three exponentials are given as dotted lines. The band is arising with rate 1 indicating the conformational change from ''off'' to ''on'' with this rate. The absorbance disappears with rate 3, indicating the ''off'' to ''on'' change with this rate. (*B*) Time-dependent absorbance changes of a marker band (in $D_2O$) for the arginine of GAP in a water environment. The amplitudes of the global fit with three exponentials are given as dotted lines. The band is decreasing with rate 2 indicating the coordination of the arginine into the binding pocket. The absorbance increases with rate 3, indicating the change back toward the water environment. (*C*) Time-dependent absorbance changes of a marker band (in $D_2O$) for the protein-bound $P_i$. This intermediate appears with the bond breakage ($k_2$) and disappears with the $P_i$-release ($k_3$).

switch-I (residues 32–38 of Ras) with $k_1$ and its reversal by $k_3$. The disappearance of the marker band at 1,589 cm$^{-1}$ (Fig. 5*B*), assigned to the arginine finger of GAP, indicates the movement of an arginine from an aqueous environment into the binding pocket with $k_2$. There is no change of arginine with $k_1$, but a change does take place with $k_2$ after switch-I is moved with $k_1$.

However, with $k_2$, we also observe at 1,192 cm$^{-1}$ (Fig. 5*C*) the bond breakage and the appearance of the protein-bound $P_i$. Because we cannot kinetically separate the movement of arginine into the binding pocket and the induced bond breakage, we have to assume that bond breakage is fast once arginine points into the binding pocket.

**Reversal of the Switch-I and Arginine Movement and $P_i$ Release with $k_3$.** The switch-I (1,684 cm$^{-1}$) and the arginine (1,589 cm$^{-1}$) reverse back with $k_3$ (Fig. 5). This cannot only be seen by the absorbance changes of the marker bands but also by the corresponding amplitude spectra. As shown in Fig. 6, the amplitude spectrum of $k_3$ is very similar to the sum of the negative amplitude spectra of $k_1$ and $k_2$. The only deviations are seen at 1,533 cm$^{-1}$ and 1,668 cm$^{-1}$. These bands, which could not be assigned as yet, are not shifted by fully labeled GAP and thus have to arise from Ras. Thus, with $k_3$, the arginine returns in the hydrophilic environment and the switch-I loop returns simultaneously to the ''off'' state as also seen in Fig. 5.

**Thermodynamic Parameters.** To determine the thermodynamic parameters of the different reaction steps, we performed the

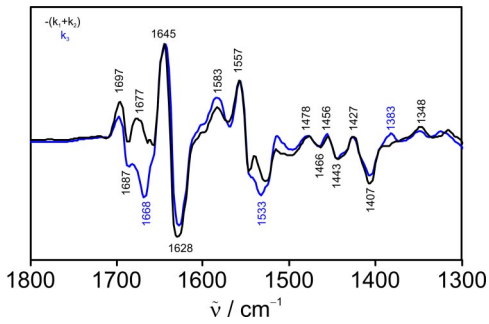


**Fig. 6.** Amplitude spectrum of rate 3 for the GTPase reaction of the Ras·GAP complex in comparison with the amplitude spectrum of the negative sum of rate 1 and rate 2. The similarity shows that the processes of rate 1 and rate 2 are reversed simultaneously with rate 3.

measurements at different temperatures to deduce the free activation energy, enthalpy, and entropy from the corresponding Arrhenius diagrams. This was performed for Ras (21) and is now extended to the Ras·GAP complex. The free activation energy for the hydrolysis of GTP in water is ≈117 kJ/mol, whereas the intrinsic GTPase reaction of Ras has a free activation energy of ≈92 kJ/mol (Fig. 7) (21). This reduction by Ras is mainly due to electrostatic interactions (21). A Ras-induced charge shift in GTP lowers the activation enthalpy from 105 kJ/mol to ≈83 kJ/mol, whereas the small entropic contributions, 12 and 10 kJ/mol, remain similar. Here, we performed analogous measurements for the GTPase reaction of the Ras·GAP complex. Whereas rate 1 was too fast to provide reliable data, we produced Arrhenius plots for the second and third rate of the GAP-catalyzed reaction (Fig. S3) as described in detail for the intrinsic reaction in ref. 21. The resulting thermodynamic scheme is shown in Fig. 7. The activation enthalpy for the cleavage reaction is similar to that of the intrinsic reaction. The ≈$10^5$-fold increase in the reaction rate and thus reduction of the free activation energy for $k_2$ is mainly due to an entropic effect. The activation entropy makes a substantially positive (favorable) contribution

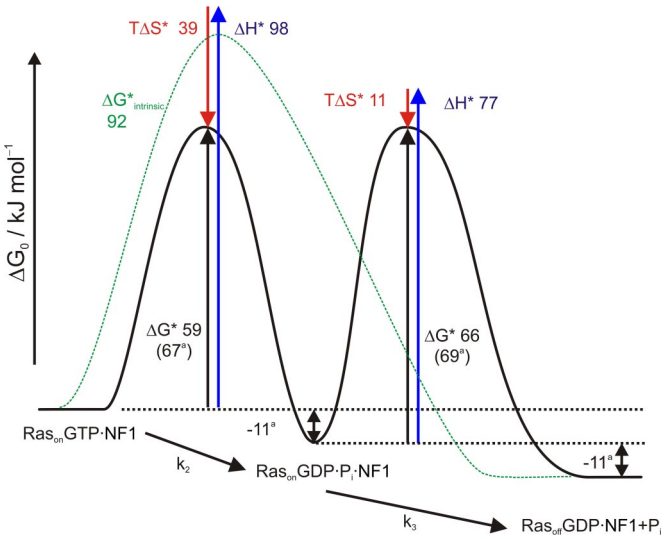


**Fig. 7.** The standard free energy diagram during the hydrolysis of GTP in the Ras·GAP complex. The enthalpic and entropic contributions to the activation free energy were determined by Arrhenius plots (*SI Experimental Procedures*). Superscript ''a'' indicates energies from ref. 42 at 303 K. The equilibrium free energy of the $P_i$ release was calculated by using 1 mM instead of 1 M as the standard. The green dotted line gives the free energy of activation for the intrinsic GTPase reaction of Ras.

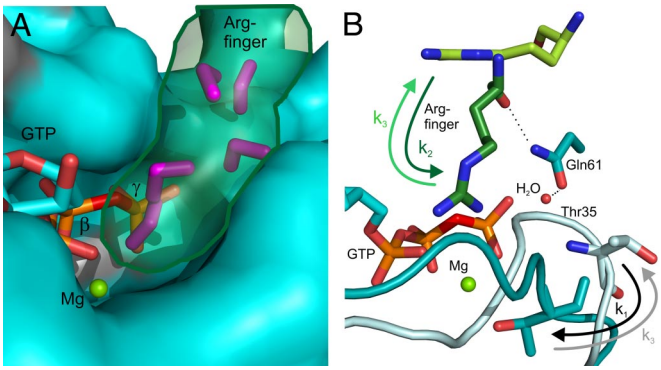


**Fig. 8.** Summary of the mechanism. (*A*) Simulations show that by the movement of the arginine (green shading) into the binding pocket of Ras·GTP (blue surface, GTP and water as stick models), approximately five structured water molecules (magenta) would be replaced (20). The release of these water molecules into the bulk would thus increase the entropy for the GTPase reaction. (*B*) Illustration of the observed processes, modeled by Protein Data Bank entries 1AM4, 1GRN, and 1QRA. With $k_1$, the conformation of switch I is changed from ''off'' to ''on'' as observed by the marker band of switch 1. With $k_2$, the arginine finger is moved into the binding pocket. The carbonyl group of the arginine-finger coordinates glutamine 61 of the switch II, which positions the nucleophilic water. With $k_3$, both processes are reversed.

with $T\Delta S_0^* = 39$ kJ/mol. In contrast, the activation entropy contribution is slightly negative in water (−12 kJ/mol) and in Ras (−10 kJ/mol). Thus, whereas catalysis due to the Ras is mostly enthalpic, the additional catalysis of the GAP is mostly entropic.

The release of inorganic phosphate and return to the ground state determined by $k_3$ has a slightly higher free activation energy, in line with the fact that is the rate-determining step of the overall reaction. The activation enthalpy of 77 kJ/mol is lower than for the $k_2$ reaction, but there is only a small favorable entropy contribution to the free energy of activation. This step is not resolved in the intrinsic reaction and thus cannot be compared.

**Positive Entropy of Activation in the Hydrolysis Step.** Most enzyme catalysis is believed to be driven by enthalpic changes (30) where the protein provides a preorganized polar environment that is stabilizing the transition state. This has been elucidated for the intrinsic GTPase reaction of Ras, where the charge distribution of GTP is shifted by Ras toward a GDP product-like state. However, there are also examples in which a positive entropy of activation contributes to catalysis (31, 32). In the case of the latter, the release of ordered (confined) water from a protein binding pocket into the bulk causes a decrease of order in the transition from the ground state toward the transition state. Here, we have to compare on one site the $Ras_{on}GTP{\cdot}GAP$ ground state, where we assume the arginine finger to be in an aqueous environment with the transition state in which the arginine is moved into the binding pocket. This compares very well the structure of Ras·GTP (or Ras·GppNHp), where the nucleotide binding site is open toward the solvent with that of the Ras·GAP complex in the transitions state mimic, where the binding site is shielded by the arginine. We can thus postulate that the arginine finger movement pushes ordered water out of the binding pocket into the bulk water. The loss of protein-bound structured water is most likely the source for a positive activation entropy $\Delta S^*$ (31). The entropy change for moving one protein-bound structured water into the bulk water is up to 8 kJ/mol (33). According to MD simulations (20), the coordination of the arginine finger with the GTP will displace approximately five water molecules (Fig. 8*A*), giving an entropy change of up to 40 kJ/mol—very similar to the experimentally observed 39 kJ/mol entropy change. The decrease of entropy due to the coordination of the arginine might be balanced by the structured waters formerly coordinating the arginine. The free energy gained by displacing the water molecules might eventually be used to induce the electrostatic interactions that stabilize the transition state for bond breakage.

## Conclusion

Our results are summarized in Fig. 8 and Scheme 2. After photolysis, the switch-I induces a surface change of Ras with $k_1$ to the ''on'' state as defined by effector binding, the arginine finger moves into the binding pocket with $k_2$, and concomitant GTP hydrolysis is observed. After hydrolysis, the protein-bound $P_i$ intermediate is still in the ''on'' conformation. With $k_3$, the switch-I movement is reversed to ''off'' and arginine moves out of the binding pocket. This implies that an efficient GAP should not only catalyze the bond breakage but also the release of the phosphate.

The positive charge of the arginine itself is largely delocalized among the guanidinium group (20). Thus, on the one hand coulomb interactions are capable of steering the arginine toward the negatively charged GTP, but on the other hand arginine alone is not able to induce a very specific charge distribution in GTP (20). The arginine finger movement changes the dielectricum in the active site by pushing waters out of the binding pocket, and the Ras-induced charge shift in GTP is increased. Any residue that can move into the binding pocket and push the waters out might thus be able to catalyze the Ras GTPase reaction. This concept can also be applied to other GTPase·GAP systems without an arginine finger and might represent a unifying concept for GAP-mediated GTP hydrolysis on G proteins.

## Experimental Procedures

Ras (residues 1–166) (34) and NF1–333 (35) were prepared with an *Escherichia coli* expression system. NF1 was expressed as a GST fusion protein with a TEV site and purified via a GSH column. The fusion protein was cleaved by the TEV-protease (36). For the $\eta^{15}N_2$-arginine labeled form of NF1, we used an optimized M9 media, in which each amino acid was added to give final concentrations of 0.834 mM. The arginine was replaced by its isotopically labeled form from Cambridge Isotope Laboratories. After the purification, the degree of incorporation and possible spreading of the labeling was quantified by mass spectrometry (37). The incorporation was >95%, and no spreading was observed. The complete $^{13}C^{15}N$-labeled form of NF1 was expressed in an *E. coli* oD2 CN medium (Silantes).

The *P*$^3$-*para*-hydroxyphenacyl ester of GTP was synthesized by coupling GDP and pHP-caged $P_i$. The latter was obtained in five steps from *para*-hydroxyacetophenone and dibenzylphosphate and according to a procedure from Park and Givens (38). For the FTIR measurements, Ras was loaded with the pHP-GTP nucleotide according to John *et al.* (39). The sample was prepared between two $CaF_2$ windows as detailed by Cepus *et al.* (40). The composition was 6 mM 1:1 complex of Ras with the caged nucleotide, 6.6 mM NF1, 25 mM $MgCl_2$, 10 mM DTT, and 200 mM Mes (pH 6).The experiments were performed at 260 K by using 12% ethylene glycol to prevent freezing. In the case of $D_2O$ measurements, the samples were resuspended five times with $D_2O$ and 12% ethylene glycol-$D_2$ was used.

Photolysis of the caged compounds was performed by an LPX 240 XeCl-excimer laser (308 nm; Lambda Physics) by 12 flashes within 24 ms. A modified Bruker IFS 66v/s spectrometer in the fast-scan mode was used for the measurement (41). The data were analyzed between 1,800 and 950 $cm^{-1}$ with a global fit

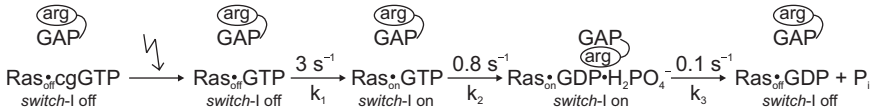


**Scheme 2.**

method (25). In this analysis, the absorbance changes $\Delta A$ were analyzed with sums of 3 exponentials with apparent rate constants $k_l$ and amplitudes $a_l$:

$$\Delta A(\nu,t) = \sum_{l=1}^{n_r} a_l(\nu) e^{-k_l t} + a_\infty(\nu).$$

In the figures, negative-amplitude spectra ($-a_l(\nu)$) are shown; the disappearing bands face downward, and the appearing bands face upward. An amplitude spectrum of the photolysis $a_0(\nu)$ is calculated by

$$a_0(\nu) = a_\infty(\nu) - \sum_{l=1}^{n_r} a_l(\nu).$$

**ACKNOWLEDGMENTS.** We thank Maryna Taranova for performing some of the Arrhenius measurements and Henrik te Heesen and Jürgen Schlitter for help with one of the figures and for fruitful discussions. This work was supported by the Ruhr University School funded by the Deutsche Forschungsgemeinschaft in the Framework of the Excellence Initiative, and by the Deutsche Forschungsgemeinschaft within the SFB 642.

1. Vetter IR, Wittinghofer A (2001) Signal transduction—The guanine nucleotide-binding switch in three dimensions. *Science* 294:1299–1304.
2. Wittinghofer A, Waldmann H (2000) Ras-a molecular switch involved in tumor formation. *Angew Chem Int Ed* 39:4192–4214.
3. Malumbres M, Barbacid M (2003) Timeline—RAS oncogenes: The first 30 years. *Nat Rev Cancer* 3:459–465.
4. Bos JL, Rehmann H, Wittinghofer A (2007) GEFs and GAPs: Critical elements in the control of small G proteins. *Cell* 129:865–877.
5. Schweins T, *et al.* (1995) Substrate-assisted catalysis as a mechanism for GTP hydrolysis of P21(Ras) and other GTP-binding proteins. *Nat Struct Biol* 2:36–44.
6. Downward J (2003) Targeting RAS signalling pathways in cancer therapy. *Nat Rev Cancer* 3:11–22.
7. Schubbert S, Shannon K, Bollag G (2007) Hyperactive Ras in developmental disorders and cancer. *Nat Rev Cancer* 7:295–308.
8. Collins I, Workman P (2006) New approaches to molecular cancer therapeutics. *Nat Chem Biol* 2:689–700.
9. Ahmadian MR, Stege P, Scheffzek K, Wittinghofer A (1997) Confirmation of the arginine-finger hypothesis for the GAP-stimulated GTP-hydrolysis reaction of Ras. *Nat Struct Biol* 4:686–689.
10. Scheffzek K, *et al.* (1997) The Ras-RasGAP complex: Structural basis for GTPase activation and its loss in oncogenic Ras mutants. *Science* 277:333–338.
11. Kosloff M, Selinger Z (2003) GTPase catalysis by Ras and other G-proteins: Insights from substrate directed superimposition. *J Mol Biol* 331:1157–1170.
12. Bourne HR (1997) G proteins—The arginine finger strikes again. *Nature* 389:673–674.
13. Egea Pascal F, *et al.* (2004) Substrate twinning activates the signal recognition particle and its receptor. *Nature* 427:215–221.
14. Focia PJ, Shepotinovskaya IV, Seidler JA, Freymann DM (2004) Heterodimeric GTPase core of the SRP targeting complex. *Science* 303:373–377.
15. Bowler MW, Montgomery MG, Leslie AGW, Walker JE (2007) Ground state structure of $F_1$-ATPase from bovine heart mitochondria at 1.9 Å resolution. *J Biol Chem* 282:14238–14242.
16. Rittinger K, *et al.* (1997) Crystal structure of a small G protein in complex with the GTPase-activating protein rhoGAP. *Nature* 388:693–697.
17. Rittinger K, Walker PA, Eccleston JF, Smerdon SJ, Gamblin SJ (1997) Structure at 1.65 angstrom of RhoA and its GTPase-activating protein in complex with a transition-state analogue. *Nature* 389:758–762.
18. Allin C, Ahmadian MR, Wittinghofer A, Gerwert K (2001) Monitoring the GAP catalyzed H-Ras GTPase reaction at atomic resolution in real time. *Proc Natl Acad Sci USA* 98:7754–7759.
19. Allin C, Gerwert K (2001) Ras catalyzes GTP hydrolysis by shifting negative charges from gamma- to beta-phosphate as revealed by time-resolved FTIR difference spectroscopy. *Biochemistry* 40:3037–3046.
20. Heesen Ht, Gerwert K, Schlitter J (2007) Role of the arginine finger in Ras-RasGAP revealed by QM/MM calculations. *FEBS Lett* 581:5677–5684.
21. Kötting C, Gerwert K (2004) Time-resolved FTIR studies provide activation free energy, activation enthalpy and activation entropy for GTPase reactions. *Chem Phys* 307:227–232.
22. Kötting C, *et al.* (2006) A phosphoryl transfer intermediate in the GTPase reaction of Ras in complex with its GTPase-activating protein. *Proc Natl Acad Sci USA* 103:13911–13916.
23. Chen XB, *et al.* (2006) A theoretical investigation of p-hydroxyphenacyl caged phototrigger compounds: An examination of the excited state photochemistry of p-hydroxyphenacyl acetate. *J Phys Chem A* 110:12406–12413.
24. Pelliccioli AP, Wirz J (2002) Photoremovable protecting groups: Reaction mechanisms and applications. *Photochem Photobiol Sci* 1:441–458.
25. Hessling B, Souvignier G, Gerwert K (1993) A model-independent approach to assigning bacteriorhodopsin's intramolecular reactions to photocycle intermediates. *Biophys J* 65:1929–1941.
26. Kötting C, Kallenbach A, Suveyzdis Y, Eichholz C, Gerwert K (2007) Surface change of Ras enabling effector binding monitored in real time at atomic resolution. *ChemBioChem* 8:781–787.
27. Barth A, Zscherp C (2002) What vibrations tell about proteins. *Q Rev Biophys* 35:369–430.
28. Garczarek F, Gerwert K (2006) Functional waters in intraprotein proton transfer monitored by FTIR difference spectroscopy. *Nature* 439:109–112.
29. Hutson MS, Alexiev U, Shilov SV, Wise KJ, Braiman MS (2000) Evidence for a perturbation of arginine-82 in the bacteriorhodopsin photocycle from time-resolved infrared spectra. *Biochemistry* 39:13189–13200.
30. Warshel A, *et al.* (2006) Electrostatic basis for enzyme catalysis. *Chem Rev* 106:3210–3235.
31. Loftfield RB, Eigner EA, Pastuszyn A, Lovgren TNE, Jakubowski H (1980) Conformational-changes during enzyme catalysis—Role of water in the transition-state. *Proc Natl Acad Sci USA* 77:3374–3378.
32. Valentine AM, Stahl SS, Lippard SJ (1999) Mechanistic studies of the reaction of reduced methane monooxygenase hydroxylase with dioxygen and substrates. *J Am Chem Soc* 121:3876–3887.
33. Dunitz JD (1994) The entropic cost of bound water in crystals and biomolecules. *Science* 264:670.
34. Tucker J, *et al.* (1986) Expression of p21 proteins in Escherichia coli and stereochemistry of the nucleotide-binding site. *EMBO J* 5:1351–1358.
35. Ahmadian MR, Hoffmann U, Goody RS, Wittinghofer A (1997) Individual rate constants for the interaction of Ras proteins with GTPase-activating proteins determined by fluorescence spectroscopy. *Biochemistry* 36:4535–4541.
36. Dougherty WG, Cary SM, Parks TD (1989) Molecular genetic-analysis of a plant-virus polyprotein cleavage site—A model. *Virology* 171:356–364.
37. Warscheid B, *et al.* (November 22, 2007) Systematic approach to group-specific isotopic labeling of proteins for vibrational spectroscopy. *Vib Spectrosc*, 10.1016/j.vibspec.2007.11.003.
38. Park C-H, Givens RS (1997) New photoactivated protecting groups. 6. p-Hydroxyphenacyl: A phototrigger for chemical and biochemical probes. *J Am Chem Soc* 119:2453–2463.
39. John J, *et al.* (1990) Kinetics of interaction of nucleotides with nucleotide-free H-ras p21. *Biochemistry* 29:6058–6065.
40. Cepus V, Scheidig AJ, Goody RS, Gerwert K (1998) Time-resolved FTIR studies of the GTPase reaction of H-ras p21 reveal a key role for the $\beta$-phosphate. *Biochemistry* 37:10263–10271.
41. Gerwert K, Souvignier G, Hess B (1990) Simultaneous monitoring of light-induced changes in protein side-group protonation, chromophore isomerization, and backbone motion of bacteriorhodopsin by time-resolved Fourier-transform infrared spectroscopy. *Proc Natl Acad Sci USA* 87:9774–9778.
42. Phillips RA, Hunter JL, Eccleston JF, Webb MR (2003) The mechanism of Ras GTPase activation by neurofibromin. *Biochemistry* 42:3956–3965.